Quench protection of the first 4 m long prototype of the HL-LHC Nb_3Sn quadrupole magnet

E. Ravaioli, G. Ambrosio, L. Bortot, P. Ferracin, S. Izquierdo Bermudez, P. Joshi, M. Maciejewski, V. Marinozzi, M. Mentink, J. Muratore, F. Rodriguez-Mateos, GL. Sabbi, E. Todesco, and A. Verweij

***Abstract*—The quadrupole magnets for the LHC upgrade to higher luminosity are jointly developed by CERN and US-LARP (LHC Accelerator Research Program). These Nb_3Sn magnets will be protected against overheating after a quench by a combination of heaters bonded to the coil outer surface and CLIQ (Coupling-Loss Induced Quench) units. The first 4 meter long prototype magnet, called MQXFAP1, was tested at the Brookhaven National Laboratory in stand-alone configuration. The magnet training campaign, consisting of 18 quenches, was interrupted due to the development of a short circuit between one heater strip and the coil. During the campaign, different quench protection schemes were implemented, including heaters attached to outer and inner layers, one CLIQ unit, and the energy-extraction system. The configuration including outer-layer heaters and CLIQ achieved the fastest current discharge, hence the lowest hot-spot temperature. The electro-magnetic and thermal transients after a quench were simulated with the program STEAM-LEDET and found in good agreement.**

***Index Terms*—accelerator magnet, circuit modeling, CLIQ, quench protection, superconducting coil.**

I. INTRODUCTION

THE UPGRADE to high luminosity of the LHC (HL-LHC) will require substituting the superconducting quadrupole magnet system close to the two high-luminosity experiments, ATLAS and CMS [1]–[3]. This system will include 150 mm aperture, two-layer, Nb_3Sn quadrupole magnets (MQXF), jointly developed by CERN and US-LARP [4]–[7]. The magnets will be manufactured in two versions with magnetic lengths of 4.2 m and 7.15 m. The main parameters of the magnet and its conductor are listed in Table I [4], [7], [8]. The magnetic field map in one magnet quadrant, calculated with a STEAM-SIGMA-generated COMSOL© model [9]–[11], is shown in Fig. 1. The peak magnetic field in the superconductor is 11.4 T.

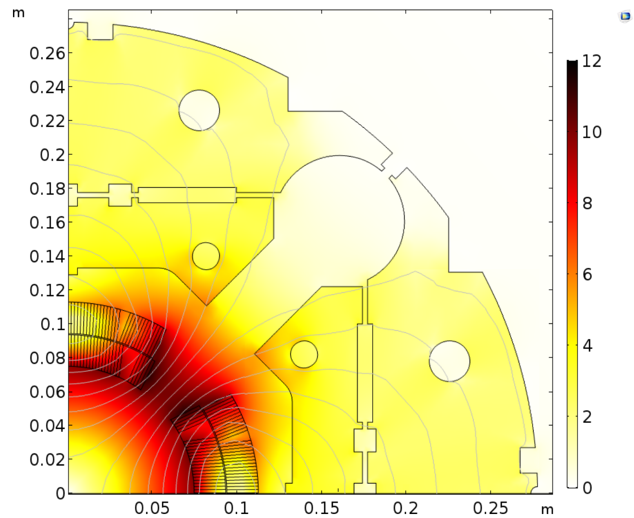

Fig. 1. High Luminosity LHC Nb_3Sn quadrupole magnet. Cross-section of one quadrant, showing the magnetic field at the nominal current of 16.47 kA calculated with a STEAM-SIGMA-generated COMSOL© model [9]–[11].

TABLE I
MAIN MAGNET AND CONDUCTOR PARAMETERS [4], [7], [8].

Parameter	Unit	Value
Nominal current, I_{nom}	A	16471
Ultimate current, I_{ult}	A	17800
Peak field in the conductor at I_{nom}	T	11.4
Operating temperature	K	1.9
Differential inductance per unit length at I_{nom}	mH/m	8.2
Stored energy per unit length at I_{nom}	MJ/m	1.2
Number of turns per pole, outer layer	-	28
Number of turns per pole, inner layer	-	22
Number of strands	-	40
Strand diameter	mm	0.85
Bare cable width, after heat treatment	mm	18.363
Bare cable thickness, after heat treatment	mm	1.594
Insulation thickness	mm	0.145

When a sudden transition to the normal state, i.e. a quench, occurs in a spot of a high energy-density superconducting coil, actions must be taken to avoid damage due to hot-spot overheating. In the HL-LHC Nb_3Sn magnets, this is particularly challenging due to the large magnet stored energy and to the relatively high margin to quench, which slows down the quench propagation. The selected protection strategy relies on an active heating mechanism, aimed at turning to the normal state most of the superconductor in a few tens of millisecond [12], [13]. In order to improve the system redundancy and effectiveness, two protection elements are included in the baseline quench protection design: heaters

Work supported by the US Department of Energy through the US LHC Accelerator Research Program (LARP) and NSFC (Contract No. 11427904).
E. Ravaioli was with the Lawrence Berkeley National Laboratory, Berkeley, CA and is now with CERN, Geneva, CH (e-mail: Emmanuele.Ravaioli@cern.ch).
P. Ferracin, S. Izquierdo Bermudez, M. Maciejewski, M. Mentink, F. Rodriguez-Mateos, E. Todesco, and A. Verweij are with CERN, Geneva, CH.
L. Bortot is with CERN and Technische Universität Darmstadt, DE.
P. Joshi and J. Muratore are with the Brookhaven National Laboratory, Upton, NY.
G. Ambrosio and V. Marinozzi are with the Fermilab National Accelerator Laboratory, Batavia, IL.
GL. Sabbi is with the Lawrence Berkeley National Laboratory, Berkeley, CA.
Manuscript received October 26, 2018.

This document was prepared by LARP collaboration using the resources of the Fermi National Accelerator Laboratory (Fermilab), a U.S. Department of Energy, Office of Science, HEP User Facility. Fermilab is managed by Fermi Research Alliance, LLC (FRA), acting under Contract No. DE-AC02-07CH11359.

TABLE II
MAIN CONDUCTOR PARAMETERS OF THE MQXFAP1 COILS [8], [34]: COPPER TO NON-COPPER RATIO, RESIDUAL RESISTIVITY RATIO, FILAMENT TWIST-PITCH $l_{\mathrm{TP,F}}$, AND STRAND TWIST-PITCH $l_{\mathrm{TP,S}}$.

Coil	Cu/no-Cu ratio	RRR[a]	$l_{\mathrm{tp,f}}$ [mm]	$l_{\mathrm{tp,s}}$ [mm]
Specifications	1.2±0.1	≥100	19±3	109±3
QXFP02	1.198-1.252	230	12-13	109
QXFP03	1.083	176	19	109
QXFP04	1.222	197	12	109
QXFP05	1.141	270	18.5	109

[a]RRR measured between 297 K and 20 K.

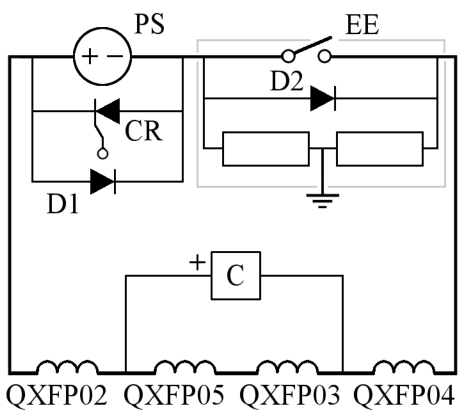

Fig. 2. Schematic representation of the magnet circuit at the BNL test facility [28], including power supply (PS), its crowbar (CR), energy-extraction system (EE), CLIQ unit (C), reverse diodes D1 and D2, and the magnet subdivided in four coils (QXFP02-QXFP05).

glued to the outer surface of the coils, and the Coupling-Loss Induced Quench (CLIQ) system [14]–[17].

Extensive quench protection studies were performed on various 1.2 m long model magnets [18]–[25], which allowed defining protection parameters [26], [27]. The first 4.0 m long prototype magnet, named MQXFAP1, was tested at the Brookhaven National Laboratory (BNL) test facility in stand-alone configuration [28], [29].

The magnet current and voltages across the coils measured during the training quenches are presented. Furthermore, the experimental results are compared to simulations performed with the LEDET (Lumped-Element Dynamic Electro-Thermal) program [14], [30], [31], which is part of the STEAM framework developed at CERN [32]. During the magnet test campaign, a short circuit developed between one coil and a heater strip, which caused the interruption of the tests [33], [34].

II. MQXFAP1 QUENCH PROTECTION

The MQXFAP1 magnet is composed of four coils (poles). The conductor parameters of each coil are summarized in Table II. A few parameters are outside specifications: the copper-to-non-copper ratio of coil QXFP03 is lower than the specified range; and the filament twist-pitches of QXFP02 and QXFP04 are lower than the specified range.

A simplified schematic of the magnet test circuit is shown in Fig. 2. A 40 mF, 500 V CLIQ unit is connected to dedicated magnet leads between poles QXFP02 and QXFP05, and QXFP03 and QXFP04. In order to reduce heat deposition in the helium bath and the consequent cryogenic recovery time, energy-extraction system (EE), composed of a switch and a 37.5 mΩ resistor, is also implemented. The middle point of the energy-extraction resistor is connected to ground.

Each coil is equipped with four copper-plated heater strips glued to its outer layer (OL-H), and two glued to its inner layer (IL-H). The nominal peak power density deposited in the heating stations is about 200 and 100 Wm^{-2} in the OL-H and IL-H strips, respectively [12], [26], [27]. Due to time constraints during the coil manufacturing process, all heater strips glued to coil QXFP03 are made of stainless-steel only, without copper plating. This increases the resistance of the heater circuit and causes a decrease of the QXFP03 heater power density of about 71%.

III. TRANSIENT DURING A TRAINING QUENCH

A total of 18 training quenches were performed during MQXFAP1 test campaigns. Different quench protection schemes were implemented to assess their performances:

- Training quenches 1-13: EE, OL-H, IL-H;
- Training quench 14: EE, OL-H, IL-H, CLIQ;
- Training quenches 15-18: EE, OL-H, CLIQ.

The triggering times of all elements of the protection system are lower than 1 ms. All training quenches occurred at currents between 15400 and 17500 A. Since the differences in the transient characteristics between different quenches are small, only two training quenches will be presented in detail.

The measured magnet transport current I_{m} [A] during the 12th training quench, occurred at a current of 16693 A, just above the nominal value of I_{nom}=16471 A, is shown in Fig. 3a. The activation of the quench protection system (t=0) was triggered 11.4 ms after the quench started. Ohmic heat is generated in the OL-H and IL-H strips, and diffused to the coil. The consequent temperature increase transfers the coil turns to the normal state, in a time comprised between 5 and 300 ms. I_{m} is discharged due to the development of electrical resistance in the coil, which reaches almost 500 mΩ at the end of the discharge. The simultaneous activation of the EE system at t=0 extracts about 21% of the magnet stored energy and causes a faster reduction of I_{m} for two reasons. First, it adds a resistance in the circuit, as observed in Fig. 2. Second, it imposes an initial current change, which causes coupling losses in the superconductor [35], [36], hence enhancing the heat deposition in it [31].

The voltages across the four coils and across the entire magnet are plotted in Fig. 3b. At t=0, the same inductive voltage is developed across all coils by effect of the EE. The coil voltages differ when resistive voltages develop in their conductor. In particular, the voltage across coil QXFP03 increases more quickly than the other coils due to its significantly lower copper fraction (see Table II), and hence higher resistance per unit length and ohmic loss per unit length. On the contrary the resistive voltage across coil QXFP02 develops less quickly than the other coils. This is partly due to the lower effectiveness of the IL-H glued to this specific coil, which was observed during the magnet initial check-out, and partly due to its higher residual resistivity ratio (see Table II).

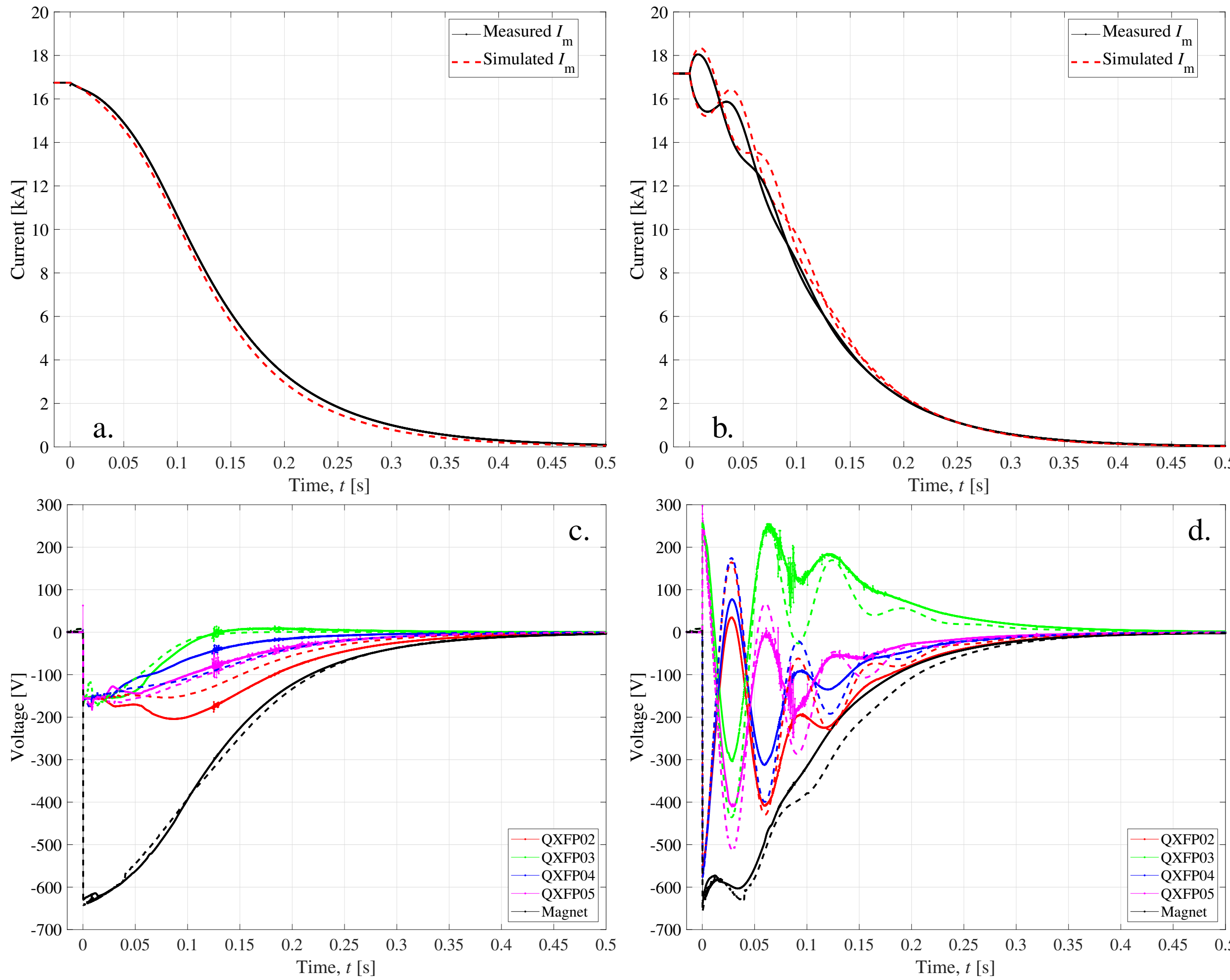

Fig. 3. Protection of the first HL-LHC Nb_3Sn quadrupole prototype after a training quench just above I_{nom}. The magnet is protected by a combination of OL-H, IL-H, and EE (a and b), or of OL-H, CLIQ, and EE (c and d). Comparison between experimental results (continuous lines) and simulations (dashed lines). a,c. Magnet transport current, versus time. b,d. Voltages across the four coils, and across the entire magnet, versus time.

The electro-magnetic and thermal transients occurring in the magnets during and after the quench are simulated with the STEAM-LEDET program [14], [30], [31]. The simulated magnet current is in good agreement with experimental results (see Fig. 3a). The simulated coil voltages are also in good agreement, with the exception of QXFP02. Note that the heater model of this coil is not corrected to account for its decreased effectiveness.

The same magnet current and voltages obtained for the 15th training quench, occurred at a current of 17168 A, with a protection scheme including EE, OL-H, and CLIQ, are shown in Figs. 3c and 3d. CLIQ imposes a positive voltage across coils QXFP03 and QXFP05, and a negative voltage across coils QXFP02 and QXFP04. The resulting current changes generate high magnetic-field changes in the superconductor, which in turn cause large inter-filament coupling loss [14], [15]. This effective heating mechanism rapidly transfers most of the coil to the normal state. As a result, the magnet current is quickly discharged. Similarly to the previously analyzed quench, the simultaneous EE triggering has an effect on the magnet discharge. In fact, it extracts about 18% of the magnet stored energy and enhances the CLIQ effectiveness due to the higher introduced current changes.

A good metric to compare the effectiveness of different quench protection systems is the quench load, defined as the time integral of the square of I_m, i.e. $\int I_m^2 \mathrm{d}t$ [A^2s]. The protection system including CLIQ reduces by 15% the quench load after the protection triggering (t>0).

The simulated fraction of coil turned to the normal state, for the two considered magnet protection options, is plotted in Fig. 4. The option EE+OL-H+CLIQ transfers about 55% of the coil to the normal state in 10 ms, compared to about 36% for EE+OL-H+IL-H. Furthermore, with the former option the entire coil is in the normal state after 50 ms, whereas with the latter option a few turns remain superconducting until 300 ms.

Simulations reproduce satisfactorily the transients (see Figs. 3c and 3d). However, the calculated quench loads differ by -3.5% and +9.6% with respect to the experimental results, for the cases EE+OL-H+IL-H and EE+OL-H+CLIQ, respectively. For the former case, the reason for the quench load underestimation is the model of the IL-H glued to coil QXFP02, which is not corrected for the observed lower heater effectiveness. Possible explanations for the quench load overestimation in the EE+OL-H+CLIQ case, already observed

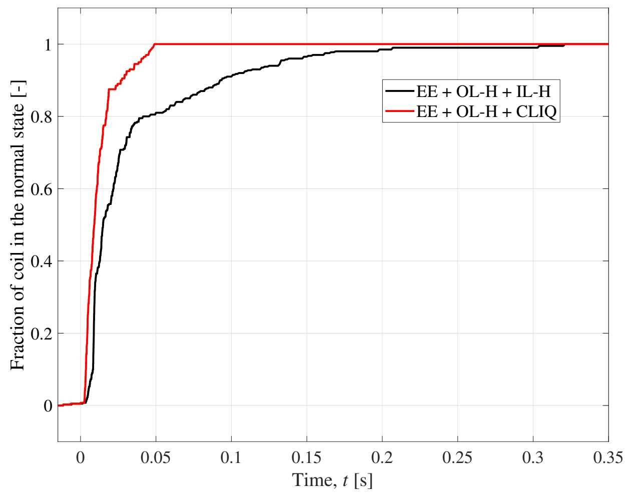

Fig. 4. Protection of the first HL-LHC Nb_3Sn quadrupole prototype after a training quench just above I_{nom}. Comparison between two quench protection options. Simulated fraction of coil in the normal state, versus time.

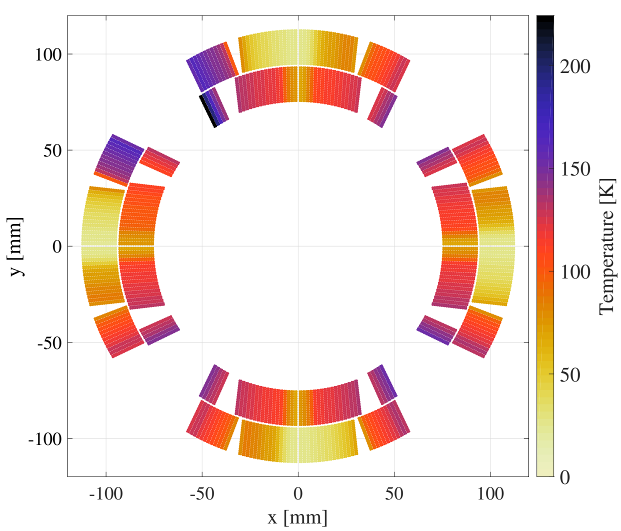

Fig. 5. Protection of the first HL-LHC Nb_3Sn quadrupole prototype after a training quench just above I_{nom}. The magnet is protected by a combination of OL-H, CLIQ, and EE. Temperature distribution in the coil cross-section at the end of the transient.

in the MQXF model magnets [26], are errors in the material properties and strand parameters, the strain-dependency of the Nb_3Sn critical current, and magnetization loss in the superconductor.

The simulated temperature distribution in the coil windings at the end of the discharge, for the EE+OL-H+CLIQ case, is shown in Fig. 5. The peak temperature, reached in the first spot to quench located in the high-field turn of an inner layer, is about 230 K, well below the acceptable limit with respect to permanent degradation of the magnet performance, which is deemed to be about 350 K [37].

The presence of the EE in the protection scheme, the non-standard heater strips glued to coil QXFP03, and the non-conform conductor properties of two coils make the results of these protection studies not fully representative of the baseline HL-LHC quench protection system.

IV. Development of a Short Circuit

The MQXFAP1 test campaign was interrupted due to failure of the coil insulation. An electrical inspection performed after the last training quench revealed that the coil was shorted to ground through one heater strip of coil QXFP05. The measured resistances were 0.5 Ω between coil and ground, and 0.5 Ω between the heater and ground, at a temperature of 1.9 K. The most likely sequence of events occurred during the test campaign is as follows:

- a short developed between coil QXFP05 and heater strip;
- a second short developed between the same coil and the same strip, thus shorting two coil turns (see R_{S2} in Fig. 2);
- during a quench, a relatively large current flew through the short, depositing significant heat in it, and damaging the coil-to-ground insulation as well (see R_{S1} in Fig. 2).

A complete analysis of the short-circuit development is described in [33], [34], together with electro-thermal simulations of a quench in the presence of a short circuit, performed with the STEAM-COSIM software[38]–[40].

V. Conclusion

The first 4.0 m long prototype magnet, named MQXFAP1, was tested at the Brookhaven National Laboratory magnet test facility. Its baseline quench protection system includes heaters glued to the coil outer-layer and CLIQ units electrically connected to the magnets.

Three different quench protection configurations are implemented and tested, including a combination of heaters glued to the coil's outer and inner layers, CLIQ, and an energy-extraction system. The magnet current and the voltages developed across its four coils are analyzed. The coil voltages during a quench discharge differ due to their different conductor properties and effectiveness of the heater strips bonded to them. The energy-extraction system, included in the protection scheme to reduce the cryogenic load during the training quench campaign, has a twofold effect on the magnet discharge. First, it extracts about a fifth of the magnet stored energy. Second, it enhances the current change, hence increasing the heat developed in the superconductor by coupling losses.

The experimental results are compared to simulations performed with the STEAM-LEDET program. Calculations are generally in good agreement with the measured signals. However, the performance of the CLIQ system is partly underestimated. In fact, the simulated quench load at nominal current is about 10% higher than the measured value.

The magnet test campaign was interrupted after the discovery of a short circuit between one coil and its heater strip, and between the strip and the ground. The authors refer to other work for a more complete analysis of this occurrence and its consequences.

Acknowledgment

The authors wish to thank Lance Cooley (NHFML), Dan Dietderich (LBNL), and Ian Pong (LBNL) for their help in collecting MQXF superconductor parameters.

REFERENCES

[1] G. Apollinari, O. Brüning, and L. Rossi, "High Luminosity LHC Project Description," CERN, Geneva, Tech. Rep. CERN-ACC-2014-0321, Dec 2014. [Online]. Available: https://cds.cern.ch/record/1974419

[2] G. Apollinari, I. Béjar Alonso, O. Brüning, M. Lamont, and L. Rossi, *High-Luminosity Large Hadron Collider (HL-LHC): Preliminary Design Report*. Geneva: CERN, 2015. [Online]. Available: http://cds.cern.ch/record/2116337

[3] E. Todesco, H. Allain, G. Ambrosio, G. Arduini, F. Cerutti, R. D. Maria, L. Esposito, S. Fartoukh, P. Ferracin, H. Felice, R. Gupta, R. Kersevan, N. Mokhov, T. Nakamoto, I. Rakno, J. M. Rifflet, L. Rossi, G. L. Sabbi, M. Segreti, F. Toral, Q. Xu, P. Wanderer, and R. van Weelderen, "A first baseline for the magnets in the high luminosity LHC insertion regions," *IEEE Transactions on Applied Superconductivity*, vol. 24, no. 3, pp. 1–5, June 2014.

[4] P. Ferracin, G. Ambrosio, M. Anerella, F. Borgnolutti, R. Bossert, D. Cheng, D. R. Dietderich, H. Felice, A. Ghosh, A. Godeke, S. Izquierdo Bermudez, P. Fessia, S. Krave, M. Juchno, J. C. Perez, L. Oberli, G. Sabbi, E. Todesco, and M. Yu, "Magnet design of the 150 mm aperture low-β quadrupoles for the High Luminosity LHC," *IEEE Transactions on Applied Superconductivity*, vol. 24, no. 3, pp. 1–6, June 2014.

[5] G. Ambrosio, "Nb_3Sn high field magnets for the High Luminosity LHC upgrade project," *IEEE Transactions on Applied Superconductivity*, vol. 25, no. 3, pp. 1–7, June 2015.

[6] E. Todesco, H. Allain, G. Ambrosio, F. Borgnolutti, F. Cerutti, D. Dietderich, L. Esposito, H. Felice, P. Ferracin, G. Sabbi, P. Wanderer, and R. V. Weelderen, "Design studies for the low-beta quadrupoles for the LHC luminosity upgrade," *IEEE Transactions on Applied Superconductivity*, vol. 23, no. 3, pp. 4 002 405–4 002 405, June 2013.

[7] P. Ferracin et al., "The HL-LHC low-beta quadrupole magnet MQXF: from short models to long prototypes," *IEEE Transactions on Applied Superconductivity*, to be published.

[8] L. D. Cooley, A. K. Ghosh, D. R. Dietderich, and I. Pong, "Conductor specification and validation for High-Luminosity LHC quadrupole magnets," *IEEE Transactions on Applied Superconductivity*, vol. 27, no. 4, pp. 1–5, June 2017.

[9] L. Bortot, M. Maciejewski, M. Prioli, A. M. F. Navarro, J. B. Ghini, B. Auchmann, and A. P. Verweij, "A consistent simulation of electrothermal transients in accelerator circuits," *IEEE Transactions on Applied Superconductivity*, vol. 27, no. 4, pp. 1–5, June 2017.

[10] L. Bortot, B. Auchmann, I. Cortes Garcia, A. Fernandez Navarro, M. Maciejewski, M. Mentink, M. Prioli, E. Ravaioli, S. Schöps, , and A. Verweij, "STEAM: A hierarchical co-simulation framework for superconducting accelerator magnet circuit," *IEEE Transactions on Applied Superconductivity*, 2017, submitted for publication.

[11] "SIGMA documentation," CERN, Geneva, Tech. Rep. EDMS 2021390, 2018.

[12] E. Ravaioli, "Quench protection studies for the High-Luminosity LHC inner triplet circuit," CERN, Geneva, Tech. Rep. EDMS 1760496, 2016.

[13] E. Ravaioli, G. Ambrosio, B. Auchmann, P. Ferracin, M. Maciejewski, F. Rodriguez-Mateos, G. Sabbi, E. Todesco, and A. Verweij, "Quench protection system optimization for the High Luminosity LHC Nb_3Sn quadrupoles," *IEEE Transactions on Applied Superconductivity*, vol. PP, no. 99, pp. 1–1, 2017.

[14] E. Ravaioli, "CLIQ," Ph.D. dissertation, Enschede, 2015, presented on 19 June 2015. [Online]. Available: http://doc.utwente.nl/96069/

[15] E. Ravaioli, V. I. Datskov, C. Giloux, G. Kirby, H. H. J. ten Kate, and A. P. Verweij, "New, Coupling Loss Induced, Quench protection system for superconducting accelerator magnets," *IEEE Transactions on Applied Superconductivity*, vol. 24, no. 3, pp. 1–5, June 2014.

[16] V. Datskov, G. Kirby, and E. Ravaioli, "AC-current induced quench protection system," Patent EP13 174 323.9, June 28, 2013.

[17] E. Todesco, "HL-LHC Decision management: WP3 - Q1/Q2/Q3 protection baseline," CERN, Geneva, Tech. Rep. EDMS 1972818, 2018.

[18] G. Chlachidze, G. Ambrosio, M. Anerella, R. Bossert, E. Cavanna, D. W. Cheng, D. R. Dietderich, J. DiMarco, H. Felice, P. Ferracin, A. K. Ghosh, P. Grosclaude, M. Guinchard, A. R. Hafalia, E. F. Holik, S. Izquierdo Bermudez, S. T. Krave, M. Marchevsky, A. Nobrega, D. Orris, H. Pan, J. C. Perez, S. Prestemon, E. Ravaioli, G. Sabbi, T. Salmi, J. Schmalzle, S. E. Stoynev, T. Strauss, C. Sylvester, M. Tartaglia, E. Todesco, G. Vallone, G. Velev, P. Wanderer, X. Wang, and M. Yu, "Performance of the first short model 150-mm-aperture Nb_3Sn quadrupole MQXFS for the High-Luminosity LHC upgrade," *IEEE Transactions on Applied Superconductivity*, vol. 27, no. 4, pp. 1–5, June 2017.

[19] S. Stoynev, G. Ambrosio, M. Anerella, R. Bossert, E. Cavanna, D. Cheng, D. Dietderich, J. DiMarco, H. Felice, P. Ferracin, G. Chlachidze, A. Ghosh, P. Grosclaude, M. Guinchard, A. R. Hafalia, E. F. Holik, S. I. Bermudez, S. Krave, M. Marchevsky, A. Nobrega, D. Orris, H. Pan, J. C. Perez, S. Prestemon, E. Ravaioli, G. Sabbi, T. Salmi, J. Schmalzle, T. Strauss, C. Sylvester, M. Tartaglia, E. Todesco, G. Vallone, G. Velev, P. Wanderer, X. Wang, and M. Yu, "Summary of test results of MQXFS1 - the first short model 150 mm aperture Nb_3Sn quadrupole for the high-luminosity lhc upgrade," *IEEE Transactions on Applied Superconductivity*, vol. 28, no. 3, pp. 1–5, April 2018.

[20] G. Ambrosio, G. Chlachidze, P. Wanderer, P. Ferracin, and G. Sabbi, "First Test Results of the 150 mm Aperture IR Quadrupole Models for the High Luminosity LHC," in *2nd North American Particle Accelerator Conference (NAPAC2016) Chicago, Illinois, USA, October 9-14, 2016*, 2016. [Online]. Available: http://lss.fnal.gov/archive/2016/conf/fermilab-conf-16-440-td.pdf

[21] H. Bajas, G. Ambrosio, A. Ballarino, M. Bajko, B. Bordini, N. Bourcey, D. W. Cheng, M. Cabon, A. Chiuchiolo, G. Chlachidze, H. Felice, L. Fiscarelli, M. Juchno, S. I. Bermudez, M. Guinchard, J. Kopal, F. Lackner, M. Marchevsky, F. Nobrega, H. Pan, J. C. Perez, H. Prin, E. Ravaioli, L. Rossi, G. Sabbi, S. S. Tavares, J. Steckert, S. Stoynev, E. Todesco, G. Vallone, P. Wanderer, X. Wang, and M. Yu, "Test result of the short models MQXFS3 and MQXFS5 for the HL-LHC upgrade," *IEEE Transactions on Applied Superconductivity*, vol. 28, no. 3, pp. 1–6, April 2018.

[22] S. Izquierdo Bermudez, "Protection studies - HCMQXFM001-CR000032," CERN, Geneva, Tech. Rep. EDMS 1836709, 2017.

[23] M. Mentink, "MQXFS3 protection studies," CERN, Geneva, Tech. Rep. EDMS xxx, 2018.

[24] M. Mentink, "Analysis of MQXFS5 CLIQ tests of November 2017," CERN, Geneva, Tech. Rep. EDMS 1930202, 2018.

[25] F. Mangiarotti et al., "Test results of the CERN HL-LHC low-beta quadrupole short models MQXFS3c and MQXFS4," *IEEE Transactions on Applied Superconductivity*, to be published.

[26] E. Ravaioli, G. Ambrosio, H. Bajas, G. Chlachidze, A. F. Navarro, P. Ferracin, S. I. Bermudez, P. Joshi, J. Muratore, F. Rodriguez-Mateos, G. Sabbi, S. Stoynev, E. Todesco, and A. Verweij, "Quench Protection Performance Measurements in the First MQXF Magnet Models," *IEEE Transactions on Applied Superconductivity*, vol. 28, no. 3, pp. 1–6, April 2018.

[27] S. Izquierdo Bermudez, G. Ambrosio, H. Bajas, N. Bourcey, G. Chlachidze, J. F. Troitino, P. Ferracin, J. C. Perez, F. Pincot, E. Ravaioli, C. Santini, S. Stoynev, E. Todesco, G. Sabbi, and G. Vallone, "Overview of the quench heater performance for MQXF, the Nb_3Sn low-β quadrupole for the high luminosity LHC," *IEEE Transactions on Applied Superconductivity*, vol. 28, no. 4, pp. 1–6, June 2018.

[28] J. Muratore, M. Anerella, P. Joshi, P. Kovach, A. Marone, and P. Wanderer, "Design and fabrication of the 1.9 K magnet test facility at BNL, and test of the first 4-m-long MQXF coil," *IEEE Transactions on Applied Superconductivity*, vol. 28, no. 3, pp. 1–4, April 2018.

[29] J. Muratore et al., "Test results of the first two full-length prototype quadrupole magnets for the LHC Hi-Lumi upgrade," *IEEE Transactions on Applied Superconductivity*, to be published.

[30] E. Ravaioli, B. Auchmann, M. Maciejewski, H. ten Kate, and A. Verweij, "Lumped-element dynamic electro-thermal model of a superconducting magnet," *Cryogenics*, pp. –, 2016. [Online]. Available: http://www.sciencedirect.com/science/article/pii/S0011227516300832

[31] E. Ravaioli, B. Auchmann, G. Chlachidze, M. Maciejewski, G. Sabbi, S. E. Stoynev, and A. Verweij, "Modeling of inter-filament coupling currents and their effect on magnet quench protection," *IEEE Transactions on Applied Superconductivity*, vol. 27, no. 4, pp. 1–8, June 2017.

[32] "STEAM website," https://espace.cern.ch/steam/.

[33] V. Marinozzi et al., "Analysis of the short-to-ground event in the LARP-AUP MQXFAP1 magnet, and its implication on the production and tests of the series magnets," *IEEE Transactions on Applied Superconductivity*, to be published.

[34] E. Ravaioli, "Analysis of the short circuit in the MQXFAP1 magnet," CERN, Geneva, Tech. Rep. EDMS 2037314, 2018.

[35] A. P. Verweij, "Electrodynamics of superconducting cables in accelerator magnets," Ph.D. dissertation, Twente U., Twente, 1995, presented on 15 Sep 1995. [Online]. Available: https://cds.cern.ch/record/292595

[36] M. Wilson, *Superconducting Magnets*, ser. Monographs on Cryogenics. Clarendon Press, 1983.

[37] G. Ambrosio, "Maximum allowable temperature during quench in Nb_3Sn accelerator magnets," in *Proceedings, WAMSDO 2013*

Workshop on Accelerator Magnet, Superconductor, Design and Optimization: CERN Geneva, Switzerland, 15-16 Jan 2013, no. FERMILAB-CONF-13-593-TD, 2013, pp. 43–46. [Online]. Available: https://inspirehep.net/record/1277941/files/arXiv:1401.3955.pdf

[38] M. Maciejewski, “Co-simulation of transient effects in superconducting accelerator magnets,” Ph.D. dissertation, Łódź, Tech. U., 2018, to be published.

[39] I. C. Garcia, S. Schps, M. Maciejewski, L. Bortot, M. Prioli, B. Auchmann, and A. Verweij, “Optimized field/circuit coupling for the simulation of quenches in superconducting magnets,” *IEEE Journal on Multiscale and Multiphysics Computational Techniques*, vol. 2, pp. 97–104, 2017.

[40] M. Maciejewski, I. C. Garcia, S. Schps, B. Auchmann, L. Bortot, M. Prioli, and A. P. Verweij, “Application of the Waveform Relaxation Technique to the Co-Simulation of Power Converter Controller and Electrical Circuit Models,” 2017.